CERN-ACC-Note-2014-0065

2014-09-08

First Considerations on Beam Optics and Lattice Design for the Future Hadron-Hadron Collider FCC

Reyes Alemany Fernandez/ BE-OP, Bernhard Holzer/ BE-ABP

Keywords: FCChh design study, lattice design

Abstract

The present document explains the steps carried out in order to make the first design of the Future Hadron-Hadron Collider (FCC-hh) following the base line parameters that can be found in [1]. Two lattice layouts are presented, a ring collider with 12 arcs and 12 straight sections, four of them designed as interaction points, and a racetrack like collider with two arcs and two straight sections, each of them equipped with two interaction points. The lattice design presented in the paper is modular allowing the same modules be used for both layouts. The present document addresses as well the beta star reach at the interaction points.

1. Introduction

Following the recommendations of the European Strategy Group, several next generation large collider projects are studied at present to carry on the investigations of the fundamental questions in high energy physics after the LHC. The future circular collider study "FCC" is investigating two possible storage ring projects, both housed in a tunnel of roughly 100 km circumference: an e+e- collider (FCC-ee) in the energy range between 90 GeV and 350 GeV and a future hadron-hadron collider (FCC-hh) with a centre of mass energy of 100 TeV.

To reach the extreme energy of the hadron-hadron collider which will carry us beyond the physics reach of the present LHC, new super conducting technologies will be needed that will allow the use of dipole magnets of up to 16 T field in Nb_3Sn magnets. As in the case of the LHC design, the machine will be optimised to accommodate two main proton experiments for highest possible luminosity (peak values of 1-5 10^{34} $cm^{-2}s^{-1}$ are aimed for) and two additional special-purpose experiments.

In this paper we summarise the first design considerations for the machine lattice and beam optics, both optimised for a circular layout as well as for an option of a racetrack-like geometry. More details about the machine parameters specification are given in Table 2 which can be found in Section 3 of [1].

2. Basic layout of the machine

Two basic configurations are studied for the ring layout:

1. A layout similar to the LHC, with arcs of equal length that are optimised for maximum dipole fill factor and that are separated by long straight sections for the installation of technical insertions and the interaction regions of the colliding beams. At present the straight sections in the ring lattice are designed for equal length

respecting ideal symmetry conditions; detailed optimisations of e.g. the collimation insertions and the beam collision and separation scheme however might lead to a slightly modified layout in the future.

2. The second option follows a racetrack-like geometry in which two long arcs, with an overall bending angle of 180^{o} each, are connected by two very long, almost straight sections. Such a layout has been proposed e.g. for the SSC design [2].

For both geometries a beam optics and optimised lattice is presented in this document, each based on fundamental modules that allow for a highly flexible design and further modifications.

Table 1

FCC-hh baseline parameters compared to LHC and HL-LHC parameters.

	LHC (Design)	**HL-LHC**	**HE-LHC**	**FCC-hh**
Main parameters and geometrical aspects				
c.m. Energy [TeV]	14		33	100
Circumference *C* [km]	26.7		26.7	100 (83)
Dipole field [T]	8.33		20	16 (20)
Arc filling factor	0.79		0.79	0.79
Straight sections	8		8	12
Average straight section length [m]	528		528	1400
Number of IPs				2 + 2
Injection energy [TeV]	0.45		> 1.0	3.3
Physics performance and beam parameters				
Peak luminosity [10^{34} $cm^{-2}s^{-1}$]	1.0	5.0	5.0	5.0
Optimum run time [h]	15.2	10.2	5.8	12.1 (10.7)
Optimum average integrated lumi / day [fb^{-1}]	0.47	2.8	1.4	2.2 (2.1)
Assumed turnaround time [h]				5
Overall operation cycle [h]				17.4 (16.3)
Peak no. of inelastic events / crossing at - 25 ns spacing - 5 ns spacing	27	135 (lev.)	147	171 34
Total / inelastic cross section σ_{proton} [mbarn]	111 / 85		129 / 93	153 / 108
Luminous region RMS length [cm]				5.7 (5.3)
Beam lifetime due to burn off [h]	45	15.4	5.7	19.1 (15.9)
Beam parameters				
Number of bunches *n* at - 25 ns	2808		2808	10600 (8900)

- 5 ns				53000 (44500)
Bunch population N[10^{11}] - 25 ns - 5 ns	1.15	2.2	1	1.0 0.2
Nominal transverse normalized emittance [□ - 25 ns - 5 ns	3.75	2.5	1.38	2.2 0.44
Number of IPs contributing to □Q	3	2	2	2
Maximum total b-b tune shift □Q	0.01	0.015	0.01	0.01
Beam current [A]	0.584	1.12	0.478	0.5
RMS bunch length [cm]	7.55		7.55	8 (7.55)
IP beta function [m]	0.55	0.15 (min)	0.35	1.1
RMS IP spot size [□m□ - 25 ns - 5 ns	16.7	7.1 (min)	5.2	6.8 3
Full crossing angle [□rad□ - 25 ns - 5 ns	285	590	185	74 n/a
Other beam and machine parameters				
Stored energy per beam [GJ]	0.392	0.694	0.701	8.4 (7.0)
SR power per ring [MW]	0.0036	0.0073	0.0962	2.4 (2.9)
Arc SR heat load [W/m/aperture]	0.17	0.33	4.35	28.4 (44.3)
Energy loss per turn [MeV]	0.0067		0.201	4.6 (5.86)
Critical photon energy [keV]	0.044		0.575	4.3 (5.5)
Longitudinal emittance damping time [h]	12.9		1.0	0.54 (0.32)
Horizontal emittance damping time [h]	25.8		2.0	1.08 (0.64)
Initial longitudinal IBS □rise time [h]* - 25 ns - 5 ns	57	23.3	40	1132 (396) 226 (303)
Initial horizontal IBS □rise time [h]* - 25 ns - 5 ns	103	10.4	20	943 (157) 189 (29)
Dipole coil aperture [mm]	56		40	40
Beam half aperture [cm]	~2		1.3	1.3
Mechanical aperture clearance at any energy at any element				>12

2.1 **Beta function at injection for FCC-hh**

One of the first questions to be answered when designing a lattice is the value of the beta function, β, at injection that can provide a beam size, which fits in the available magnet aperture. Estimations of the expected dipole and quadrupole fields of the new Nb_3Sn magnets for a given aperture have to be combined with the resulting beam dimensions for a lattice cell.

Using the LHC injection parameters as scaling examples, the biggest beam size σ that has to be accommodated in the beam pipe can be calculated as

$$\sqrt{\varepsilon\beta} = 1.1mm \tag{1}$$

where we refer to the normalised design emittance of ε = 3.5 μm at injection and β = 180 m in the LHC arcs.

The LHC effective aperture dimension for a magnet coil at 293 K in the LHC standard quadrupoles is 56 mm diameter. Taking into account the additional restrictions of the beam screen, the available aperture is reduced to 44.04 mm in one direction and 34.28 mm in the other and accordingly, the smallest aperture in LHC at injection energy corresponds to 14σ.

Following this value as reference for the FCC-hh design, the basic arc cell has to be optimised taking into account the expected magnet aperture, the beam emittance at 3.3 TeV injection energy and the beta function that can be optimised via the layout of the FODO cells in the arc.

The magnet coil aperture for FCC-hh magnets is expected to be 40 mm in diameter for the highest available gradient. Scaling the expected magnet gradient with the aperture need, a number of values is obtained as guide line for this design. They are summarised in Table 2 [3]. Compared to the LHC magnets the available aperture in FCC-hh is reduced by a factor of 40/56. Requiring still

$$\left(\frac{r}{\sigma}\right)_{FCC} = \left(\frac{r}{\sigma}\right)_{LHC} = 14 \tag{3}$$

the maximum tolerable value for the FCC beam size, $\sigma_{FCC,}$ at injection would be:

$$\sigma_{FCC} = \frac{r_{FCC}}{r_{LHC}}\sigma_{FCC} = \left(\frac{40mm}{56mm}\right)1.1mm = 0.79mm \tag{4}$$

and the value of the corresponding maximum beta that has to be provided by the lattice can be calculated.

The emittance at injection will depend on the injection energy. Table 3 shows the different emittance values for the different injection energies that are being discussed at present and the corresponding maximum beta values that can be accepted in the ring.

Table 2

Current estimated quadrupole gradient for Nb_3Sn technology according to [3].

Gradient (T/m)	Diameter (mm)	Pole tip field (T)
450	40	9
370	50	9.25
320	60	9.6

Table 3

Optimized beta values for the different possible injection energies: In each case at least 14σ aperture are obtained as minimum free aperture requirement in the future FCC magnet coil.

E_{inj} (TeV)	1	1.5	2	2.5	3	3.5	4	4.5	5
ϵ (10^{-10}m rad)	35.2	23.5	17.6	14.1	11.7	10.1	8.8	7.8	7.0
β (m)	217.7	326.5	435.3	544.2	653	761.8	870.7	979.5	1088.3
Lcell (m)	127.5	191.3	255	318.8	382.5	446.3	510.0	573.8	637.5

The minimum injection energy is defined by the available pre-accelerator on one side and the field quality of the high-energy ring magnets on the other side, when operated at the injection energy and during the first steps of the acceleration. If the same ratio of injection to full energy as for the LHC is assumed, the FCC-hh injection energy would be around 3.3 TeV. For this injection energy, the maximum beta value that guaranties sufficient aperture at injection is of the order of 700 m. In the following calculations injection energy of 3 TeV and beta function of 600 m are considered in order to introduce a bit of margin.

2.2 Basic cell length

Once the maximum beta function is determined and assuming for obvious reasons a phase advance of 90^o per cell, the cell length, L, can be calculated:

$$\hat{\beta} = \frac{\left(1+\sin\frac{\varphi}{2}\right)L}{\sin\varphi}, \qquad \breve{\beta} = \frac{\left(1-\sin\frac{\varphi}{2}\right)L}{\sin\varphi}. \tag{5}$$

Table 3 compiles the resulting values for the cell length for different beta functions and beam energies.

2.3 Bending angle and total number of dipoles

The bending angle of the main dipoles depends on the beam rigidity and the integrated dipole length of the machine. It can be calculated with the formula:

$$\alpha = \frac{\oint Bdl}{p/e} \approx \frac{16T \cdot 14.3m}{50 \cdot 10^{12} eV/e\, 3 \cdot 10^8 m/s} \approx 1.37 mrad \tag{6}$$

where 16 T dipole field and 50 TeV per beam have been assumed as specified in [1]. Assuming a magnetic length of 14.3 m, as the current LHC dipoles, we obtain a minimum number of dipoles needed for the FCC-hh:

$$N_b = \frac{2\pi}{\alpha} = 4689 \tag{7}$$

2.4 Number of dipoles per cell and fill factor

FCC-hh foresees 12 straight sections with a length of around 1.4 km each. The total ring circumference is expected to be of the order of 100 km; therefore 83.2 km are available for the arcs and should be covered to the maximum possible integrated dipole length to aim

for highest beam energy. Out of this 83.2 km available for the arc design, the space needed for dipole-dipole and dipole-quadrupole interconnections has to be subtracted. For the time being the values corresponding to the LHC are taken into account and they are compiled in Table 4. In LHC two different distances between dipole and quadrupole exist: l_s = 1.06 m and l_l = 3.67 m; in order to provide the additional space needed for these interconnections in Nb_3Sn technology the longer drift is assumed on both sides in the present design.

Table 4

Dipole-dipole interconnection, dipole-quadrupole interconnection, dipole and quadrupole length for LHC.

L_{dip} (m)	14.3
L_{qua} (m)	3.1
$L_{dip\text{-}dip}$ (m)	1.36
$L^{max}_{dip\text{-}qua}$ (m)	3.67

In order to compute the optimum number of dipoles per cell, a cell length L_{cell}, has to be assumed, for example, 350 m which would fit for 3 TeV injection energy according to Table 3. As sketched in Figure 1, the FODO cell starts and ends in the middle of a focusing quadrupole and contains one defocusing quadrupole in between. In between the quadrupoles, the number of dipoles that can be allocated is determined only on their foreseen length:

$$\frac{L_{cell} - 2L_{quad} - 4L_{dip-quad}}{L_{dip}} = \frac{350 - 6.2 - 14.68}{14.3} = 23.02 \tag{8}$$

Since an even number of dipoles is needed, 22 dipoles could fit in the given space, 11 at each side of the defocusing quadrupole. Now, the $L_{dip\text{-}dip}$ space for the dipole-dipole connections has to be considered in order to make sure there is enough space left to fit the interconnection space between dipoles. In this configuration there are N_{dip}-1 spaces dipole-dipole, i.e. 21x$L_{dip\text{-}dip}$ = 28.56 m. The following calculation should be made to assess this last question and fix the maximum number of allowed dipoles:

$$L_{cell} \geq 2L_{quad} - 4L_{dip-quad} - 22L_{dip} - 21L_{dip-dip} \tag{9}$$

As can be calculated, the right hand side of the inequality is bigger than L_{cell}, thus only 20 dipoles can be fitted in the given L_{cell}. Evaluating again Eq. 9 for 20 dipoles, 350 m ≥ 332.72 m, is obtained.

Thus either the cell length is fixed to 332.72 m or 350 m are kept and 17.28 m are left as contingency in case more space is needed for the technical layout of the quadrupole-dipole or dipole-dipole interconnections, or in case dipoles longer than 14.3 m are technically feasible.

The dipole fill factor for the chosen configuration is:

$$\eta = \frac{\Sigma L_{dip}}{L_{cell}} = 81.7\% \tag{10}$$

Following the symmetry conditions of the ring design, a total number of cells for the ring of 240 cells will be needed, each containing 20 dipoles, summing up to an overall number of bending magnets needed for the arc lattice of 4800 dipoles.

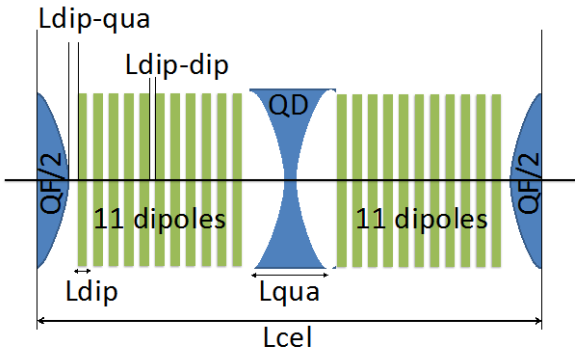

Figure 1 An example of a FODO cell with a total of 22 dipoles.

The cells will be equally distributed over the arcs and taking into account the required length of the long straight sections, L_{lss}=1.4 km, that will connect the 12 arcs, the circumference of the complete ring will add up to 100.8 km.

In order to obtain the optimum fill factor for a given single cell length a variety of different cell designs has been compared and summarised in Table 5. The table also shows the corresponding number of optimized dipoles per cell, total number of dipoles in the ring and achievable beam momentum. The information is summarised in the plot of Figure 2.

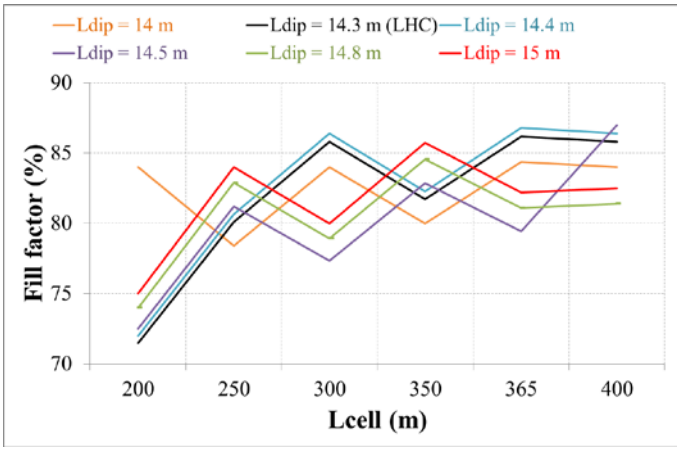

Figure 2 Fill factor for different values of dipole length and different cell lengths.

Table 5

Number of optimized dipoles per cell, total number of dipoles in the ring, fill factor and beam momentum for different values of dipole length and different cell lengths. The total number of dipoles assumes all the cells in the arc are normal arc FODO cells. Later on it will be seen that insertion cells are needed for dispersion suppression and matching section. These two types of cells contribute with half the number of dipoles in the case of dispersion suppression and zero dipoles in the case of the matching section.

Lcell (m)	200	250	300	350	365	400
β (m)	341	427	512	598	623	683
Ldip (m)	14					

Ndip opt/cell	12	14	18	20	22	24
Ndip tot	4992	4662	4986	4760	5016	4992
η (%)	84	78.4	84	80	84.38	84
p (TeV/c)	53.42	49.87	53.42	50.87	53.66	53.42
Ldip (m)	14.3					
Ndip opt/cell	10	14	18	20	22	24
Ndip tot	4160	4662	4986	4760	5016	4992
η (%)	71.5	80.08	85.8	81.71	86.19	85.8
p (TeV/c)	45.47	50.93	54.56	51.96	54.81	54.56
Ldip (m)	14.4					
Ndip opt/cell	10	14	16	20	20	24
Ndip tot	4160	4662	4986	4760	5016	4992
η (%)	72	80.64	86.4	82.29	86.8	86.4
p (TeV/c)	45.79	51.31	54.88	52.39	55.21	54.94
Ldip (m)	14.5					
Ndip opt/cell	10	14	16	20	20	24
Ndip tot	4160	4662	4432	4760	4560	4992
η (%)	72.5	81.2	77.33	82.85	79.45	87
p (TeV/c)	46.11	51.67	49.12	52.75	50.54	55.33
Ldip (m)	14.8					
Ndip opt/cell	10	14	18	20	20	24
Ndip tot	4160	4662	4432	4760	4560	4576
η (%)	74	82.88	78.93	84.57	81.1	81.4
p (TeV/c)	47.06	52.74	50.13	53.85	51.58	51.76
Ldip (m)	15					
Ndip opt/cell	10	14	16	20	20	22
Ndip tot	4160	4662	4432	4760	4560	4576
η (%)	75	84	80	85.71	82.19	82.5
p (TeV/c)	47.69	53.45	50.81	54.57	52.28	52.46

3. Defining the lattice modules for MADX

In the following, the different lattice modules that have been defined in MADX to build the different layouts are listed. The H in the quadrupole names indicates “half quadrupole”. DRIFT46 is a 46 m drift space between the IP and Q1 for the experimental insertion. DRIFTQ3Q4 is the drift between the Q3 and Q4 quadrupoles. The “R” and “L” appearing in the module names indicate if the module is to the right or the left of the IP.

3.1 IP drift

IPR: DRIFT46, Q1FH
IPL: DRIFT46, Q1DH

3.2 Mini-beta insertion

ITR: Q1FH, Q2D, Q3FH
ITL: Q1DH, Q2F, Q3DH

3.3 Drift between mini-beta insertion and the first matching section:

DRIFTR: Q3FH, DRIFTQ3Q4, Q4DH

DRIFTL: Q3DH, DRIFTQ3Q4, Q4FH

3.4 Matching section for the mini beta insertion

MS1R: Q4DH, Q5F, Q6DH
MS2R: Q6DH, Q7F, Q8DH
MS1L: Q4FH, Q5D, Q6FH
MS2L: Q6FH, Q7D, Q8FH

3.5 Dispersion suppression for the mini beta insertion

Half bend solution for 90o phase advance.
DS1R: Q8DH, 6 HALF BEND DIPOLES, Q9F, 6 HALF BEND DIPOLES, Q10DH
DS2R: Q10DH, 6 HALF BEND DIPOLES, Q11F, 6 HALF BEND DIPOLES, QDH
DS1L: Q8FH, 6 HALF BEND DIPOLES, Q9D, 6 HALF BEND DIPOLES, Q10FH
DS2L: Q10FH, 6 HALF BEND DIPOLES, Q11D, 6 HALF BEND DIPOLES, QFH

3.6 Arc cells

Arc cells starting with QD: QDH, 6 DIPOLES, QF, 6 DIPOLES, QDH
Arc cells starting with QF: QFH, 6 DIPOLES, QD, 6 DIPOLES, QFH

3.7 Dispersion suppression for the insertion regions other than mini beta

DS_IRF: QFH, 6 HALF BEND DIPOLES, QD, 6 HALF BEND DIPOLES, QFH
DS_IRD: QDH, 6 HALF BEND DIPOLES, QF, 6 HALF BEND DIPOLES, QDH

3.8 Matching section for the insertion regions other than mini beta

MS_IRF: QFH, QD, QFH
MS_IRD: QDH, QF, QDH

The modules defined in this way allow, as well, building either a symmetric mini-beta lattice around the IP, or anti-symmetric (like the case of LHC).

4. LHC-like ring accelerator

Based on the results presented in Table 5, the following parameters have been considered to build the first version of a ring accelerator. To start with, a factor 2 with respect to LHC is considered in terms of cell length. The dipole length has been fixed to 14.2 m. The values of Table 5 in grey have been considered and are summarized below.

The number of cells per arc is indicated in Fig. 3. The ring has a total circumference of 99130 m. The length of the mini beta insertions including the dispersion suppression and matching section cells is 1783.106 m. The length of the insertion regions (IR) for collimators, radio-frequency cavities, injection and extraction lines is 1248.84 m, including dispersion suppression and matching section cells. The arc on the right hand side of the IP contains 32.5 FODO cells. The half-cell is needed to switch from a FODO cell to a "DOFO" cell and regain the symmetry of the optics. The arc on the left hand side of the IP needs 32 FODO cells. The arcs in between IRs contain 34 FODO cells.

Lcell $_{(\sim 2\text{xLcell-LHC})}$ = 208.14 m
Ndip/cell = 12
Ncell/arc = 34
Ndip = 5016
Ldip = 14.2 m
Lqua = 5.17 m
β arc = 350 m
p = 50 TeV
r = 20 mm
η=82%

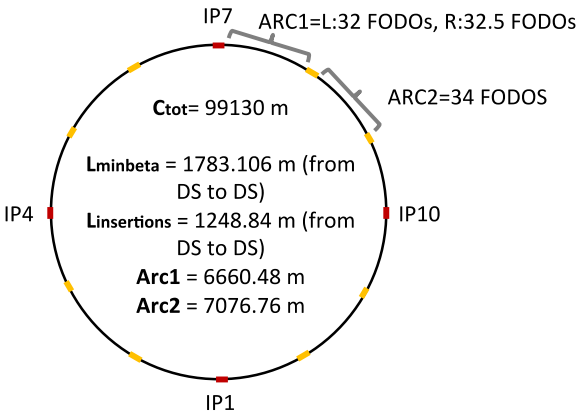

Figure 3 Layout of the LHC like ring version.

4.1 Lattice and beam optics

At present all quadrupoles (except the mini-beta quadrupoles, Q1-Q3) have the same length of 5.17 m which has been chosen to respect the gradient value of Table 2 for an aperture radius of 20 mm. Figure 4 shows the beta function and the dispersion for a single basic arc cell. In Figure 5 the beam optics of the right hand side of the IR is shown, including the lattice structure. It consists out of the mini-beta triplet, Q1-Q3, the matching section, Q4-Q8, and the dispersion suppressor, where in addition to the half bend scheme the quadrupoles Q9-Q11 are installed to obtain some flexibility in the lattice design. The complete anti-symmetric beam optics in a FCC-IR region is presented in Figure 6.

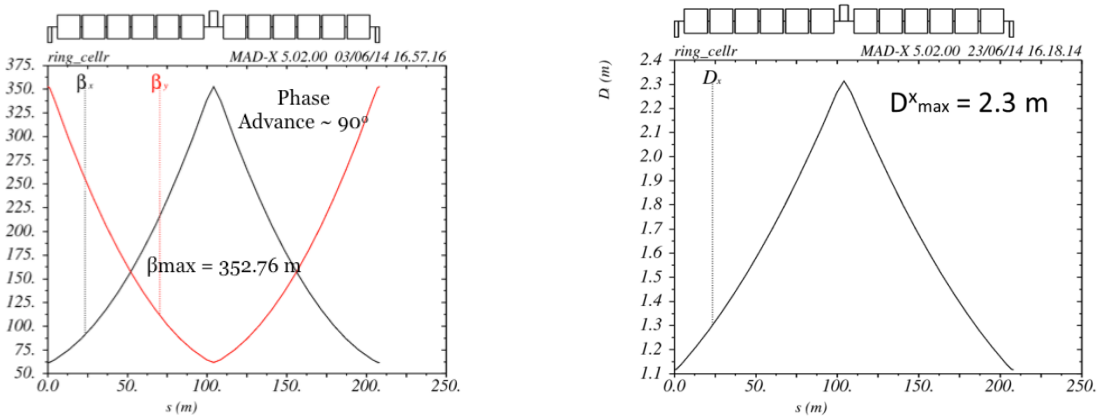

Figure 4 Left: beta function and, right: dispersion, for an arc FODO cell with 90° phase advance.

Following the aperture requirements at the mini beta triplet where the β-function reaches its maximum, the length of the quadrupole lenses has to be increased considerably to provide the necessary focusing strength. For the three mini-beta quadrupoles Q1, Q2 and Q3, 13 m, 30 m and 13 m long devices will be needed. Those lengths respect the available gradient (Table 2) for a radius of 20 mm. The quadrupoles Q1 to Q11 are independently powered as they have to provide the large aperture need in the triplet, the matching section and the flexibility in the dispersion suppressor region, respectively. The beta value at the interaction point is 1.1 m following the design parameter list [1]. The maximum of the beta function occurs naturally at the mini-beta quadrupoles and it is of the order of 9 km.

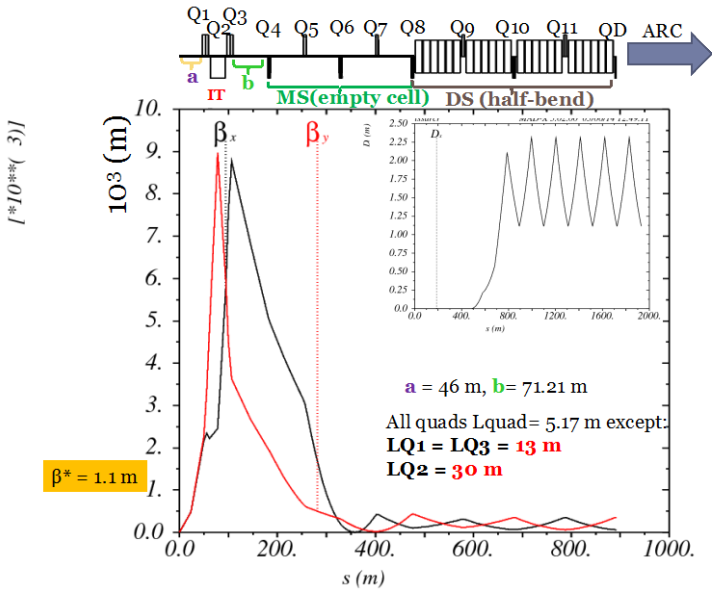

Figure 5 Beta function and dispersion for the right hand side of an insertion region with mini-beta quadrupoles for a beta value at the interaction point of 1.1 m [1]. Q1 to Q11 are independently powered quadrupoles. QD is the main lattice defocusing quadrupole.

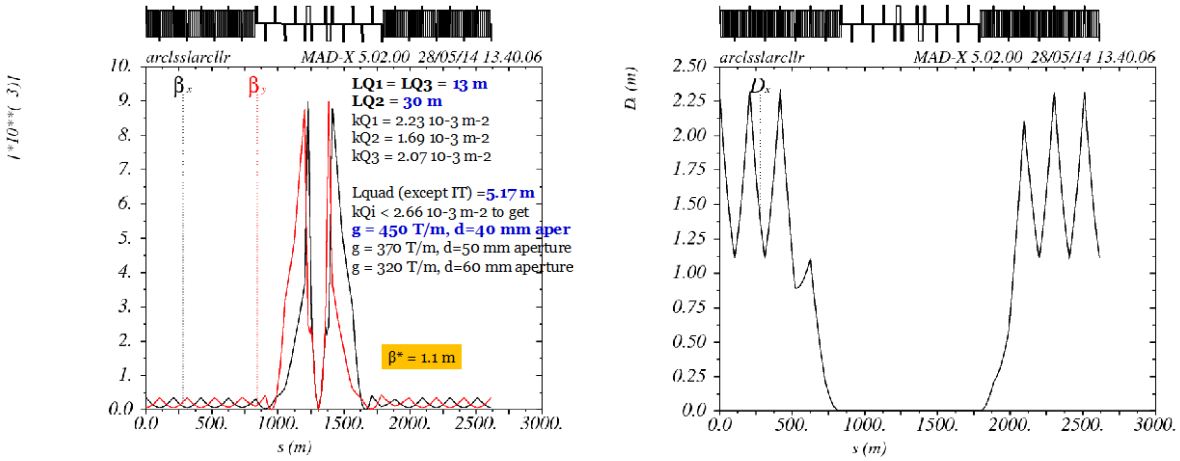

Figure 6 Left: beta function around an insertion region with mini-beta quadrupoles for β* = 1.1 m [1]. The maximum of the beta function, ~ 9 km, occurs at the mini-beta quadrupoles. Right: dispersion around the insertion region with mini-beta quadrupoles.

For symmetry reasons the complete ring is built out of 12 arcs, connected by 12 identical long straight sections. Four of them will be designed as mini-beta insertions for the installation of the particle detectors, the remaining eight straight sections will provide the space needed for the RF system, beam diagnostics, injection and extraction and they will provide the lattice flexibility for the optics modifications that are needed to install e.g. the collimation system.

The optics of the complete ring is shown in Figure 7. The left plot shows the hor. and vert. beta function, the right part the dispersion. The regular pattern of the dispersion suppressors to create dispersion free straight sections is clearly visible in the figure.

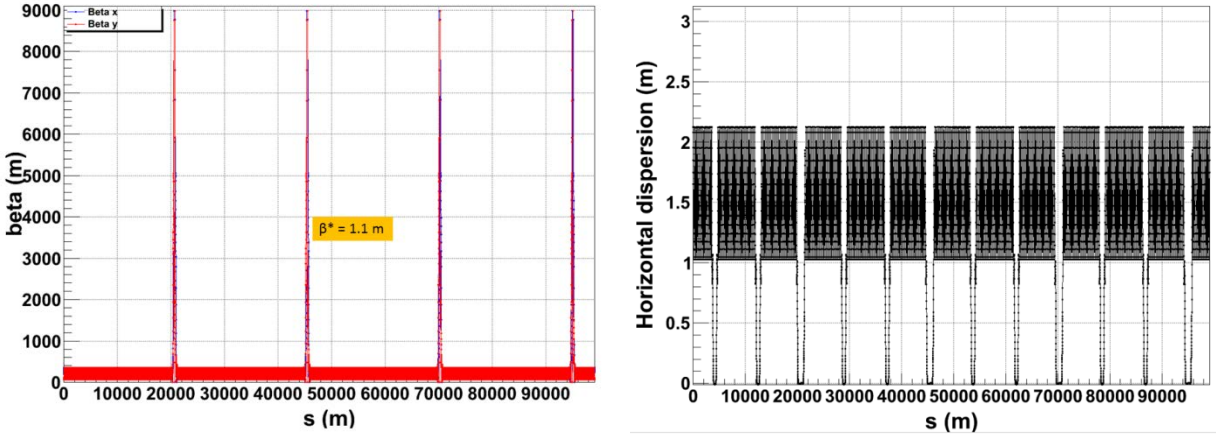

Figure 7 Left: beta function for the whole ring for a β* = 1.1 m. Right: dispersion function for the whole ring. Dispersion vanishes at the 12 insertion regions.

4.2 Aperture considerations

First aperture considerations have been studied for this LHC-like geometry, assuming a 40 mm diameter coil aperture of the magnets, and 2.2 μm rad normalized emittance for 25 ns [1]. The beam size and the available physical aperture (without tolerances and errors included) are calculated and shown in Figure 8.

It should be emphasised that these numbers will only serve as first estimates and more precise investigations have to follow including the design of the vacuum chamber, the beam screen and possible optics and orbit tolerances. Still, however, at present a bare aperture of ±30 σ is obtained inside the triplet quadrupoles, compared to the situation of the LHC triplets where for the same assumptions and, again, without the additional restrictions resulting from the beam screen a value of ±23 σ is obtained.

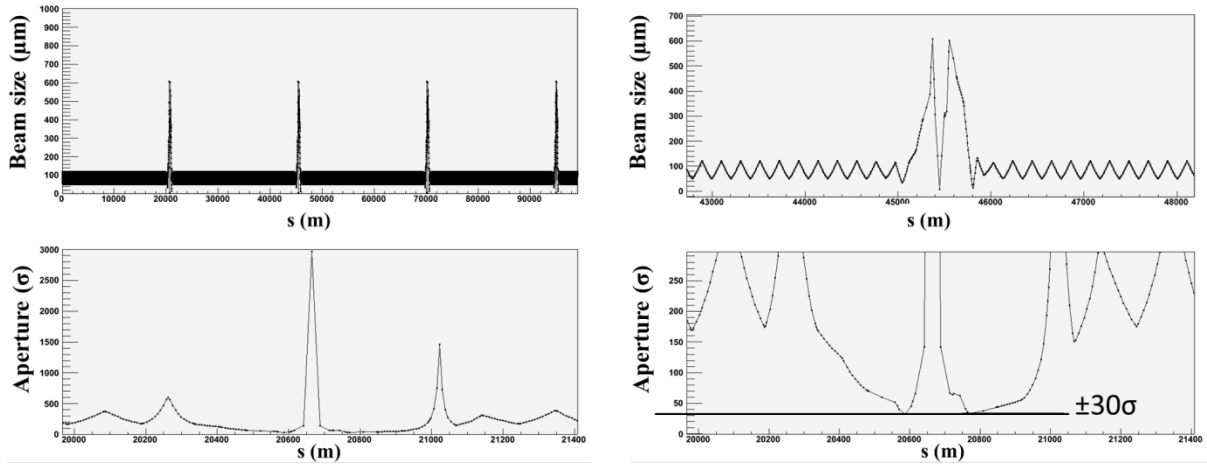

Figure 8 Calculated beam size and aperture for the ring of Fig. 7. The aperture refers to an inner bore radius of the magnets of 20 mm. At the mini-beta quadrupoles where the beam size reaches its highest value, an aperture of ±30 sigma is obtained.

Table 6 shows the strengths of the different independent powered quadrupoles that are used in the matching section and the dispersion suppressor region. As already mentined above, a magnetic length of 5.17 m is assumed for every magnet, except for the mini beta triplet lenses where due to the increased aperture need longer quadrupole are required. At present, the strengths of the quadupoles Q7 and Q8 are still beyond the hardware specifications of Table 2.

Table 6

Strengths of the different independent powered quadrupoles for a magnetic length of 5.17 m.

Q4D	-2.77630e-04	Q4F	3.13e-04
Q5F	1.27198e-03	Q5D	-1.3e-03
Q6D	-1.45778e-03	Q6F	1.25e-03
Q7F	5.93102e-03	Q7D	-5.98e-03
Q8D	-3.39691e-03	Q8F	3.51e-03
Q9F	2.33514e-03	Q9D	-2.23e-03
Q10D	-2.30692e-03	Q10F	2.61e-03
Q11F	2.63780e-03	Q11D	-2.53e-03

In order to reduce their gradients, a re-iteration will be needed, combined eventually by an increased length of these quadrupoles. Following a simple scaling of the integrated gradient the following values are obtained:

For $k^{Q7F}{}_1$=5.93 10^{-3} m^{-2}, l_1=5.17 m --> $k^{Q7F}{}_2$=2.66 10^{-3} m^{-2}, $l^{Q7F}{}_2$= 11.5 m.
For $k^{Q7D}{}_1$=-5.98 10^{-3} m^{-2}, l_1=5.17 m --> $k^{Q7D}{}_2$=2.66 10^{-3} m^{-2}, $l^{Q7D}{}_2$=11.6 m.
For $k^{Q8D}{}_1$=-3.4 10^{-3} m^{-2}, l_1=5.17 m --> $k^{Q8D}{}_2$=2.66 10^{-3} m^{-2}, $l^{Q8D}{}_2$= 6.6 m.
For $k^{Q8F}{}_1$=3.51 10^{-3} m^{-2}, l_1=5.17 m --> $k^{Q8F}{}_2$=2.66 10^{-3} m^{-2}, $l^{Q8F}{}_2$= 6.8 m.

5. Optics for different values of β*

The FCC design parameter list assumes a value of the amplitude function of β* = 1.1m. And the optics that has been optimised and presented in Figure 7 refers to this design value. However, provided enough aperture in the triplet magnets is available, where the beta function reaches its local maximum, the interaction region layout can be used to match for a variety of different, namely smaller β* values. In a range of β*=0.25 m ... 1.1 m a set of beam optics has been established and plotted in Figure 10 for comparison. In each case the optics has been re-matched to the periodic solution of the arc lattice.
The actually reachable β* value that can be obtained, and as a consequence the resulting luminosity will depend mainly on the available magnet aperture in the triplet region. The aperture estimations for each beam optics - within the same assumptions made for the design optics of β*=1.1m - is shown in Figure 11.

A zoomed view of the triplet region, where the aperture requirements are most stringent is shown in Figure 12. For the smallest β* values (25cm) a free aperture of ±15.5 σ is obtained, which might be too small to be considered a safe scenario.

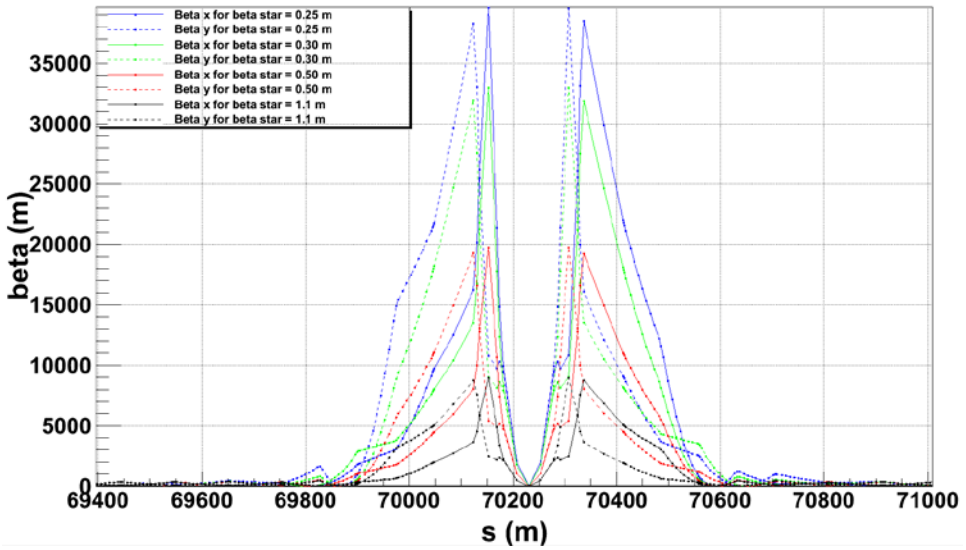

Figure 10 Beta functions for different values of β*: 0.25 m, 0.30 m, 0.50 m and 1.1 m.

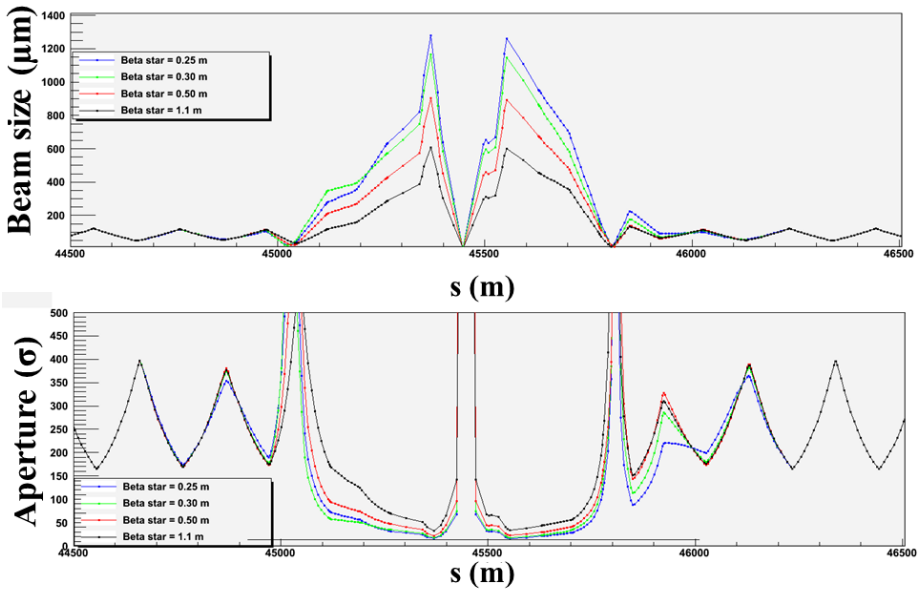

Figure 11 Calculated beam size and aperture for the different beta functions of Fig. 10. The values refer to 20 mm quadrupole aperture radius.

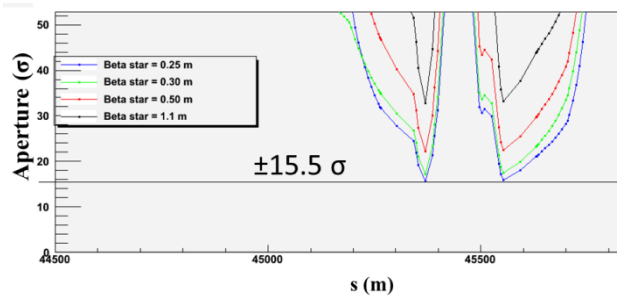

Figure 12 Zoom of the aperture for the different beta functions of Fig. 11. The minimum value obtained, ±15.5σ, corresponds to β* = 0.25 cm.

6. Race track geometry

Currently for the overall layout of the FCC-hh collider two main geometries are being discussed: A ring-type version, as presented in the first part of this paper, and a racetrack-like version. While in the ring design the 12 arcs are connected by 12 dispersion free straight sections to install the hardware for injection, extraction, collimation systems for momentum and betatron cleaning, and finally the four experiments, the racetrack geometry combines these issues in two long straight sections. The design of the 8.4 km long straights will be a task of its own: Among the usual boundary conditions for the beam optics required e.g. for an efficient beam collimation, a serious input arises from the fact that two interaction points will be located one after the other in the same dispersion free beam line. Strictly speaking therefore these insertions are not fully straight, as debris resulting from the beam collisions in one IP should not reach the second detector located downstream.

The advantage of the racetrack design however will be that instead of the space consuming dispersion suppressor and matching regions on both sides of the 12 arcs in the ring design, the arcs can be optimised for highest dipole fill factor and only the two long straights are equipped with the additional matching sections for the mini-beta insertions and the dispersion suppressors. Using the modules described in Sec. 3, it is straight forward to design a racetrack version equivalent to the ring version and only a slight re-matching of the optics is needed to obtain a valuable solution. The geometry of the racetrack design is shown in Figure 13. In the present design the two interaction points that share the same long straight section are located at the very end of the corresponding arcs. However, following the needs from other installations a re-shuffling is possible without problems, as every module that has been designed for the machine layout - like mini-beta, dispersion suppressor, dipole free cells, etc, represents a fully matched system that can be installed at whatever place in the ring.

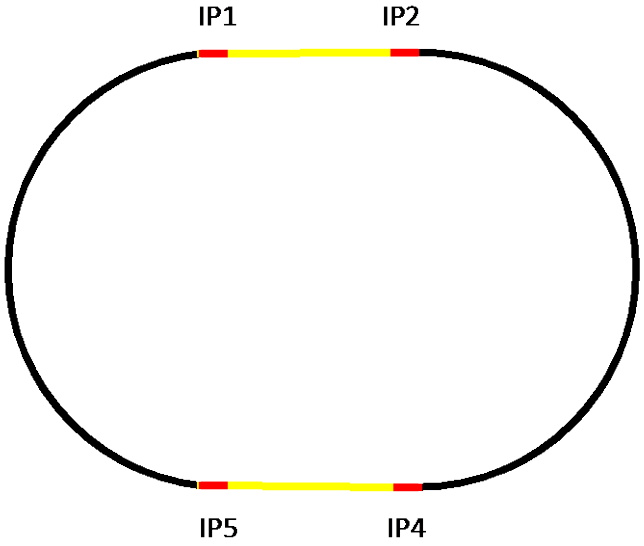

Figure 13 FCC-hh racetrack layout. The total accelerator length in this case is 100.8 km, the straight sections are 7416.802 m long each and the arcs are 46689.311 m long each.

Referring as before to the design parameter list [1], a mini-beta insertion with $\beta^* = 1.1$ m has been introduced at four positions in the lattice. Figure 14 and 15 show the overall beam optics (i.e. the beta function in horizontal and vertical plane) and the horizontal dispersion function. By definition of the racetrack geometry the dispersion free regions now are considerably longer than in the ring design and are clearly visible in the plot.

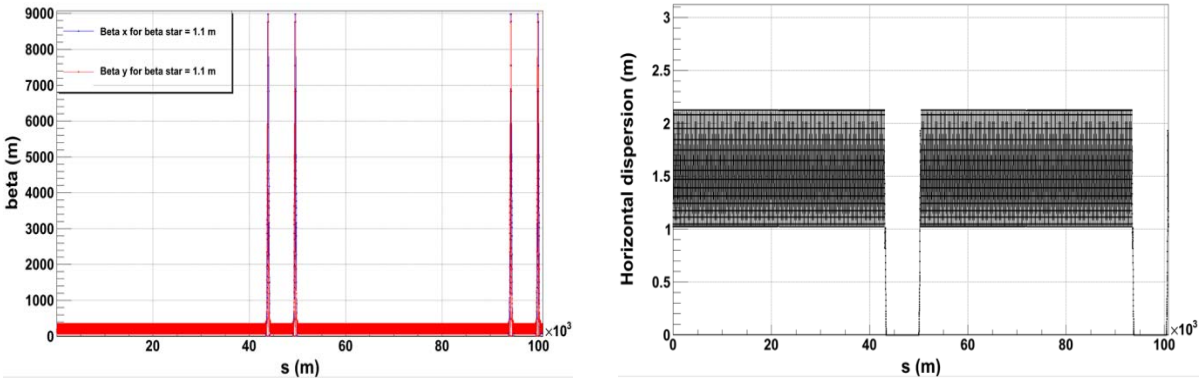

Figure 14 Left: beta function for the whole racetrack ring for a β* = 1.1 m at the interaction points. Right: dispersion function for the whole racetrack ring. The dispersion vanishes at the two insertion regions.

Since the same insertion regions as for the ring-geometry are used for the racetrack, the same considerations about reachable beta star values, discussed in Sec. 7, apply again.

Figure 15 shows a zoomed view of the 7.4 km long straight section, which will house the two experiments and at the same time the complete machine equipment that is distributed in the ring like design over the twelve straight short sections.

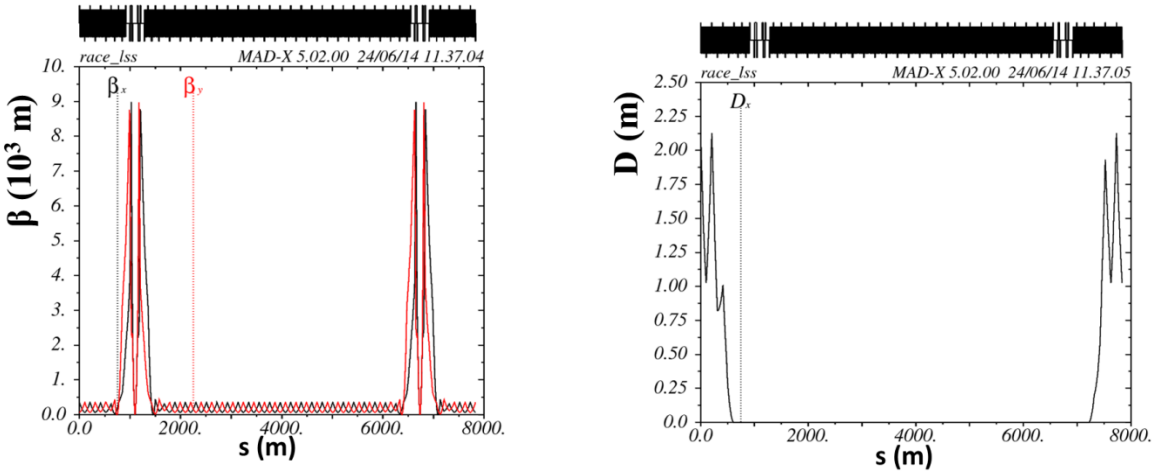

Figure 15: Left: beta function of the 7.4 km long straight section. The β* at the IP is 1.1 m. Right: dispersion for the 7.4 km long straight section.

7. Next steps

To avoid background problems from the debris that is produced in one interaction region and that could reach the second detector, located downstream in the same long straight section, a small angle between the two interaction regions will have to be introduced and dipole magnets will have to be installed to deflect the beam locally. To avoid undesired contributions to the dispersion function in the rest of the machine this will be done using a non-dispersive deflection scheme, where the unavoidable dispersion is compensated right after the last local dipole magnet.

The long straight sections then will have to be optimised according to the boundary conditions set by the different insertions. While in the ring design each straight section is equipped with a sufficient number of individually powered matching quadrupoles, the long straights of the racetrack design might need additional matching quadrupoles to optimise the beam optics for the installation of the different insertions.

In both cases, the ring as well as the race-track version of the FCC-hh collider, the present status has been saved and the relevant information for the lattice structure, the magnet strengths and the MADX command file have been stored in the FCC database [4] to make them available for further optimisation and use of the FCC study group.

8. Conclusions

Two lattices for the FCC-hh collider were studied, following the present design conditions of a ring like and a racetrack like geometry. In both cases the lattice is built out of a number of basic optics modules, that are combined to form a valuable lattice and beam optics. The basic FODO cell in the arcs is optimised for maximum feasible dipole length and dipole fill factor, forming a 200 m long cell with 90 degrees phase advance in both planes. Dispersion suppressors have been designed, using the half bend scheme, which is most adequate for the chosen phase and they are combined with matching sections that are flexible enough for a variety of different optics conditions at the future interaction point.

The magnet strengths used in the beam optics follow the first estimates for the new Nb_3Sn technology which is foreseen for dipole and quadrupole magnets of the storage ring and only in a few cases a slight re-iteration will be needed to get a technically feasible design.

References

[1] A. Ball et al., “Future Circular Collider Study Hadron Collider Parameters”, EDMS doc. 1342402.

[2] M. Syphers, “Review: Superconducting Super Collider, Optics Design and Layout”, https://indico.cern.ch/event/317384/

[3] Internal communication by Ezio Tedesco.

[4] FCC project database, /afs/cern/ch/eng/fcc/hh/LATTICE_V3/